BIF003W/2-068875-73
HEXAGON Cy 1
5 February 1973
Sheet Count: 73

7-0124-73
Cy 1

FLIGHT TEST ENGINEERING ANALYSIS REPORT
FOR
THE HEXAGON PROGRAM SATELLITE VEHICLE NUMBER FOUR (S)

Prepared and Submitted by the
Satellite Vehicle Integrating Contractor

J. W. Chapman
J. W. Chapman
Assistant Program Manager

HANDLE VIA BYEMAN
CONTROL SYSTEM ONLY

FOREWORD

This report describes the performance of the fourth HEXAGON Program Satellite Vehicle (SV-4). The vehicle was launched on 10 October 1972 and after a 69 day primary mission and a 22 day SOLO mission was deboosted on Rev 1463 on 8 January 1973.

This report does not explicitly cover the SOLO mission; however, results from SOLO are used as appropriate when they contribute substantially to the understanding of primary mission events.

CONTENTS

(b)(1)
(b)(3)

ABBREVIATIONS

ACS	Attitude Control System
ARM	Attitude Reference Module
BV	Booster Vehicle
ECS	Extended Command System
EDAP	Electrical Distribution and Power
ESD	Emergency Shutdown
FCEA	Flight Control Electronics Assembly
FDU	Failure Detector Unit
FOSR	Flexible Optical Solar Reflector
F/S	Forward Section
FT	Film Transport
FTFD	Field Test Force Director
H/S	Horizon Sensor
IRA	Inertial Reference Assembly
IV	Isolation Valve
MCLR	Master Clear Off
MCS	Minimal Command System
MMC	Martin Marietta Corporation
MOP	Manual Operation
MS	Mid Section
M/S	Mid Section
OA	Orbit Adjust
O^2A^2	On-Orbit Attitude Adjust
OAS	Orbit Adjust System
OB	Optical Bar
PACS	Primary Attitude Control System

PFA	Post Flight Analysis
PGR	Pitch Gyro Rate
P/L	Payload
PIP	Predicted Impact Point
PMU	Programmable Memory Unit
QCM	Quartz Crystal Microbalance
RACS	Redundant Attitude Control System
RC	Recovery Capsule
RCS	Reaction Control System
REA	Reaction Engine Assembly
REM	Reaction Engine Module
RV	Re-entry Vehicle
SBAC	Satellite Basic Assembly Contractor
SCO	Sub Carrier Oscillator
SECO	Stage II Engine Cut-Off
SGLS	Space-Ground Link System
SPC	Stored Program Command
SRM	Solid Rocket Motor
SS	Sensor System
SV	Satellite Vehicle
TM	Telemetry
TMV	Telemetry Volt
TT&C	Tracking, Telemetry and Command
VTT	Vandenburg Targeting Team

Section 1
SUMMARY OF GENERAL SYSTEM PERFORMANCE

1.1 SV MISSION PERFORMANCE

The SV-4 was injected into a nominal 89 by 150 nm orbit on 10 October 1972 by a Titan IIID Booster Vehicle. The initial orbit was 85 by 156 nm; however, the nominal orbit was established on the first OA. Ascent events were all nominal and proper stabilization of the SV allowed deployment of the Solar Arrays on the first rev. The Subsatellite was properly ejected on Rev 2. The four RVs were separated from the SV with their film loads on mission days 12, 27, 45 and 69. All RVs were successfully recovered in the air. Following an extended SOLO operation period (which is not described in this report), the SV was successfully deboosted on Rev 1463 in the 91st day on orbit. The performance of the SV with respect to the primary mission objectives is summarized for each of the four mission segments as follows.

<u>Segment One</u>

Operational photography began on Rev 5 after successful completion of the Sensor Subsystem (SS) health checks. The SS was operated with constraints of zero rewind and scan center angles of 0, ±15 and ±30 degrees to preclude mistracking as had occurred during the SV-3 mission. All subsequent SS operations throughout RV-1 demonstrated nominal characteristics except for improper stowing of the Optical Bars (OB's) after some early operations. This anomaly was traced to the software which was effectively corrected by Rev 91 and proper OB stowing was consistently obtained thereafter. On Rev 119, the focus of both cameras was adjusted on the basis of on-board diagnostics. Approximately 28,300 feet of film per camera (including prelaunch footage) was exposed and stowed in RV-1 which was recovered on Rev 180. Post-flight analysis (PFA) showed the overall quality of the acquired photography good to very poor in both cameras. There was a definite correlation between the very poor sections and improper OB stowing.

Segment Two

Operational photography exhibiting nominal characteristics continued with the same constraints imposed during RV-1. On Rev 228 the focus of both cameras was again adjusted, this time on the basis of RV-1 PFA. Engineering tests confirmed proper On-Orbit Attitude Adjust (O^2A^2) settings. Approximately 29,040 feet of film per camera was exposed and stowed in RV-2 which was recovered on Rev 423. PFA showed the overall quality of acquired photography improved over that of RV-1. PFA also revealed a ruptured RV pyro battery with subsequent spotting of some of the film, and the presence of loose metallic and glass phenolic particles.

Segment Three

Operational photograpy progressed normally until Rev 474 when an ESD occurred on the A-side (forward looking) camera. Successful recovery was established by a health check on Rev 495.

A brief period of B side (aft looking) camera mono operation ensued prior to the resumption of stereo photography on Rev 508, when the zero rewind constraint was lifted. A 5-inch per second rewind was used for all subsequent operations and nominal characteristics were exhibited for the remainder of RV-3. Approximately 27,006 feet of A side camera film and approximately 27,665 feet of B side camera film were exposed and stowed in RV-3 which was recovered on Rev 715. PFA on the A-side film in the region of the ESD occurrence confirmed the probable cause of the ESD being a drag of a roller or capstan near the input of the fine film drive as was indicated by the on-board diagnostics. Also discovered were: an A side film tear in the region of the Rev 640 operation occurring on forward moving exposed film; and more debris of a RV relay panel with some fragments interleaved in the film stacks. Neither produced discernable disturbances in operation, overall quality of acquired photography was slightly less than that of RV-2 with no difference pre/post ESD detected.

Segment Four

The SS exhibited nominal performance throughout this segment except that on Rev 778 an A side camera interlock source signal failed. Successful operation was resumed with the disabling of verification circuitry. Preparation for use of the 10,000 feet of color film at the end of the A side supply began on Rev 888 and continued until the resumption of stereo photography on Rev 898. A side camera focus, O^2A^2 and exposure curves were adjusted and a temporary constraint on scan center, progressively relaxed to pre-color values by Rev 960, were imposed. On Rev 1088 an SV yaw error developed and SS Vy and O^2A^2 adjustments were made in an attempt to correct for the error. The last 8 photographic operations were run with the SS thus biased. A-side camera film was depleted triggering an ESD on Rev 1101. ESD was disabled and the end of A side film and all but approximately 40 feet of B side film were stowed in RV-4. Approximately 23,260 feet of A side film (including the entire 10,000 feet of color) and approximately 25,640 feet of B side film were exposed and stowed in RV-4 which was recovered on Rev 1105.

During PFA, RV debris was again found in the stacks and severe damage to the film of the last two operations on each camera was observed as the result of RV-4's pyro battery rupturing. Although the quality of some of both black-and-white and color photography was good, the bulk of coverage was only fair primarily due to poor weather, snow cover and low sun angles and the overall quality was slightly lower than that of RV-3. The best color frame was subjectively judged to have a resolution of 2.5 feet.

SOLO Phase

The SOLO phase extended from Rev 1106 to deorbit on Rev 1463. SOLO objectives were:

a. Demonstrate 75 day life of the SBA and subsystems. This was later extended to 90 days.

b. Perform a list of SOLO experiments.

Having accomplished these objectives, the flight was terminated on Rev 1463.

The results of the SOLO experiments and the evaluation of data obtained will be presented in a SOLO report.

1.2 SUBSYSTEM PERFORMANCE

Performance of the SV Subsystem met all requirements throughout the mission except for the for the anomalies developed in the ACS. Subsystem performance is summarized as follows.

Attitude Control System (ACS)

Although vehicle attitude and rate control was maintained, a yaw bias developed on ACS 2 on Rev 564 which resulted in transfer to ACS 1 on Rev 582. A yaw bias developed in ACS 1 on Rev 1088 which disappeared on Rev 1102. A failure in the FCEA caused the vehicle to pitch up and tumble following the separation of RV-4 on Rev 1105; however, recheck of the data indicates this failure occurred between Rev 940 and Rev 973. There was also noise in the ACS 1 IRA pitch gyro channel from Rev 170 to Rev 350 that may have pulsed the RCS but otherwise did not influence the system.

2 D/D

Reaction Control System (RCS)

As expected, leakage developed on RCS 1 which gradually increased until transfer to RCS 2 was necessary on Rev 413. No leakage developed on the RCS 2 throughout the remainder of the flight.

Orbit Adjust System (OAS)

The OAS performed nominally throughout the mission.

Tracking, Telemetry and Command (TT&C)

With the observance of the antenna pattern recommendations, the TT&C system met all requirements.

Electrical Distribution and Power (EDAP)

The EDAP system performed normally throughout the mission.

Lifeboat II (LB-II)

The LB-II system performed normally throughout the mission. An experiment showed the Lifeboat II system adequate to check vehicle attitude during an inertial RV separation. Potential Lifeboat II control for deboost was verified by using it for control on Rev 1210.

Thermal Control

All active and passive thermal control designs performed within requirements. Evaluations of the ascent contamination and the RV retro plume impingement were successful. The extensive use of FOSR in lieu of white silicone paint and the need for a shield for the Quantic equipment on SV-8 were substantiated by these tests.

Structures and Mechanisms

All performance requirements were met.

A more detailed discussion of these subsystems is presented in subsequent sections of this report.

1.3 ANOMALY SUMMARY

Significant anomalies and malfunctions are listed chronologically in Table 1-1. The list includes a description of the anomaly, the mission consequences, the changes indicated for subsequent vehicles and a cross-reference to the appropriate paragraphs where detailed discussions may be found.

TOP SECRET / H

Table 1-1

ANOMALIES

Day	Description	Impact	Cross Reference Paragraph
1	Right Solar Array Deployment Delayed	No effect on mission. Cage mechanism revised for SV-5.	14.2
1	Delayed Station Acquisition	No impact on basic mission. Modulation indexes will be adjusted on SV-5 to increase downlink real-time performance.	4.2.2
1	Improper OB Stowage	Large corrector plate temperature change. Corrected by day 6 by modifying software.	7.3
11	PACS Pitch Rate Noise	No effect on mission. Disappeared on day 22. Attributed to components used in IRA pitch channel. Component upgrading in process. EFFECTIVITY SV5 ↑ UP	2.1.8
12	RV-1 One of Eight Heavy Lead Lines Broken	No effect on mission. Slack members abrade loaded lines. Adequate strength remains.	8.3
12	RCS-1 REM Leak	No effect on mission. Primary REM valves started to leak as expected. Switched to RCS 2 on day 26 and completed flight using OAS propellant. Same tanking arrangement will be used for SV-5.	2.2 and Subparagraphs
27	RV-2 Retro Truss Separation Delayed	No impact on RV performance. Redesign from shear pins to controlled separation plane on all future RVs.	8.3
27	Pyro Battery 2 Failure	Electrolyte spotted outer wraps of stack. Redesigned internal vents on all future RV batteries.	8.3
27	Three of Eight Heavy Lead Lines Broken	Same as RV-1.	8.3

13

TOP SECRET / H

BIF003W/2-068875-73

Table 1-1 (Cont.)

Day	Description	Impact	Cross Reference Paragraph
30	ESD on Side A Looper carriage contacted travel limit switch	P/L ops resumed on day 32. Drag of roller or capstan near input of fine film drive.	7.1
35	RACS Yaw Bias Offset	Transfer M2V2 to M1V2 on day 36. P/L results on Rev 567 were poor. No P/L ops Rev 570 to Rev 582. Attributed to short in torquer circuit inside gyro. Testing augmented. Design changes under study.	2.1.5
48	A-Side Interlock source signal failure	Verification circuitry disabled to complete mission	7.3
58	PACS FCEA Failure	No impact on basic mission. Not discovered until vehicle tumbled after RV-4. Attributed to inoperative hybrid integrated buffer switch.	2.1.6
68	PACS Yaw Bias Offset	Offset disappeared on Rev 1102. P/L ops continued with SS Vy and O^2A^2 adjustments. Similar to RACS Yaw Bias Offset. See Referenced paragraph.	1.1 Segment 4, 2.1.5 and 7.3
68	ESD on Side A Film Depletion	Normal with supply depletion as confirmed by flight data. ESD disabled and end of film stowed.	7.1
69	RV-4 Relay Panel Epoxy Cover Failure	Pieces retrieved in both RV-4 and RV-3, some interleaved in film stacks. Under investigation. Interim fix by taping epoxy on relay panels.	8.3

BIF003W/2-068875-73

Section 2

ATTITUDE CONTROL

2.1 ATTITUDE CONTROL SYSTEM

The SV-4 Attitude Control System (ACS) experienced four anomalies during the mission. Except for these anomalies the ACS performed as expected. The summaries presented in this section detail those requirements that could be verified from flight data. The performance of the control force equipment is reviewed in subsection 2.2.

2.1.1 BV/SV Separation

BV/SV separation was completed at approximately 545.5 seconds vehicle time. (Vehicle time starts 67 sec before lift-off.) Master clear-off (MCLR), which enables the pitch, roll and yaw integrators to accumulate angle, was at 513.4 sec and SECO, which terminates BV attitude control, occurred at 533.6 sec vehicle time. The SV attitude changes from SECO to BV/SV separation and the attitude and rates as measured at BV/SV separation are shown in Table 2-1. Also, the times in which the SV attitudes and rates came back within the specified limits following BV/SV separation (capture) are shown in Table 2-1.

Table 2-1

BV/SV-4 SEPARATION

	Rate and Attitude at BV/SV Separation						Capture			
	Rate (deg/sec)		Attitude (degrees)				Attitude		Rate	
			H/S at Sep		Δ (SECO-Sep)					
	Specified	Actual	Specified	Actual	Specified	Actual HS/Int	Specified (1) (deg)	Actual (2) (sec)	Specified (3) (deg/sec)	Actual (4) (sec)
Pitch	±.752	-.159	-21.7 to +13.0	+1.3	±3.5	-0.50/ -0.74 (5)	±0.70	661.3	±.014	99
Roll	±.786	-.241	±10.6	+1.0	±3.0	+0.52/ +0.60	±0.70	661.3 +520	±.021	661.3
Yaw	±.752	+.175	-11.4 to +11.1	–	+4.5 to -3.5	– /+1.82	±0.64	661.3 +520	±.014	661.3

(1) Attitude in degrees to be achieved in 1500 sec.

(2) Actual time required to achieve specified attitude (switch to fine mode plus settling time).

(3) Rate in degrees/second to be achieved in 1500 sec.

(4) Actual time required to achieve specified rate

(5) Relative to the local horizontal

2.1.2 Subsatellite/SV Separation

The Subsatellite/SV Separation took place on Rev 2.9 at 13994.6 sec with the vehicle in the nose forward attitude. The ACS parameters just prior to the instant of separation were as follows:

Event	Actual	Specified
Pitch H/S	-0.4 deg	±1.0 deg
Roll H/S	-.04 deg	±1.0 deg
Roll Integrator	-.06 deg	
Yaw Integrator	+.04 deg	
Pitch Integrator	+.11 deg	
Roll Gyro Rate	0 deg/sec	±0.1 deg/sec
Pitch Gyro Rate*	-.069 deg/sec	±0.1 deg/sec
Yaw Gyro Rate	0 deg/sec	±0.1 deg/sec

The maximum SV rates observed following the yaw separation impulse were:

Pitch Gyro Rate*	-.072 deg/sec
Roll Gyro Rate	-.080 deg/sec
Yaw Gyro Rate	-.044 deg/sec

With the Subsatellite located on the vehicle +Y side and along the -Z axis at Z = -11.47 in., a negative roll rate such as shown above was expected.

2.1.3 Payload Operations

SV rate and attitude requirements during payload operations were met with the exception of those listed in Table 2-2. The yaw gyro rate bias (discussed in Section 2.1.5) resulted in roll and yaw attitudes outside the pointing requirements of 0.70 and 0.64 deg degrees respectively. The yaw gyro rates shown in Table 2-2 are the bias rates of the anomalous controlling IRA and are not the actual vehicle rates. Rate performance was met at all times.

*Geocentric program rate of -0.0687 deg/sec was included.

Table 2-2

P/L OPS DURING YAW GYRO BIAS PERIODS

Rev	FT + Vehicle Time (sec)	FT - Vehicle Time (sec)	Yaw Gyro Rate (deg/sec)	Approximate Yaw Attitude (deg)	Roll Attitude (deg)
567.4	504104.0	504127.2	-.008	+2.2	+0.5
1093.4	789090.6	789147.0	+.012	-3.3	-0.85
1094.4	794467.8	794492.8	+.011	-3.0	-0.8
1095.4	799733.8	799770.4	+.012	-3.3	-0.85
1096.3	804976.2	805078.6	+.012	-3.3	-0.85
1097.4	810550.2	810566.8	+.013	-3.6	-0.9
1100.6	827613.2	827635.2	+.013	-3.6	-0.9
1101.4	831868.8	831941.0	+.013	-3.6	-0.9
1101.4	832055.4	832083.2	+.013	-3.6	-0.9
1102.4	837271.8	837288.4	0	0	0

Since no yaw attitude sensor is available, the yaw attitude is estimated from the following relationship:

$$\psi_\epsilon = -\frac{H_\phi}{\omega_o H_\psi} \omega_{z_g}$$

where

ψ_ϵ = Yaw attitude

H_ϕ = Roll H/S to Roll gain = .0055

ω_o = Orbital rate = .0012 rad/sec

H_ψ = Roll H/S to yaw gain = .0167

ω_{z_g} = Yaw Gyro Rate

2.1.4 Recovery

The pitch-down maneuvers preceding the RV separations were all within specification and are summarized in Table 2-3, and the RV separation performance summary is shown in Table 2-4.

Following separation of RV-4, vehicle control was lost. Details of the failure are discussed in Section 2.1.6. Subsequent tumbling capture details are covered in Section 2.1.7. Separation of RV-4 from the satellite vehicle was completed before loss of control.

Table 2-3

PITCH-DOWN PERFORMANCE PRECEDING RV SEPARATION

RV/Rev	Pitch-Down Angle		Maneuvering Time to 0.1 deg/sec		Pitch-Down Coast Rate		
	Desired ±3.0 deg	Actual (PDWN)	Specified (sec)	Actual (sec)	Command Rate (deg/sec)	Coast Rate Expected (deg/sec)	Coast Rate Actual (PGR) (deg/sec)
1/180.3	-37.9	-37.5	150	68	-0.705	-.75 ±.05	-0.70
2/423.3	-40.9	-41.2	150	85	-0.705	-.75 ±.05	-0.70
3/715.3	-41.7	-40.8	150	70	-0.705	-.75 ±.05	-0.73
4/1105.3	-41.5	-39.8	150	70	-0.705	-.75 ±.05	-0.74

Table 2-4

SUMMARY OF RV/SV SEPARATION PERFORMANCE

RV/Rev	Peak Pitch Rate (deg/sec)	Max Pitch Integrator Angle (deg)	Induced Impulse by RV (lb-sec)	Pitch-Down Prior to Separation (deg)	Pitch-Up Following RV Sep to Removal of Manvr Cmd (deg)	Pitch Inertia (After Sep) (slug-ft^2)	Pitch Thruster Moment Arm (ft)	Roll Spec (deg)	Angle Meas H/S (deg)
1/180.3	2.24	14.1	133	-37.5	99.2	99040	29.0	±1.0	+0.16
2/423.3	2.31	16.2	125	-41.2	99.4	76222	24.5	±1.0	+0.30
3/715.3	2.39	17.7	127	-40.8	99.3	61358	20.1	±1.0	+0.20
4/1105.3	(1)	(1)	(1)	-39.8	(1)	51730	15.4	±1.0	(1)

(1) See discussion Section 2.1.6

TOP SECRET / H

TOP SECRET / H

2.1.5 IRA Bias Anomalies

The yaw rate bias offset was seen on IRA 1012 (PACS) starting at Rev 1088 and on IRA 1009 (RACS) starting at Rev 564. Probable cause is a high impedance short from the torquer circuit to the case inside gyros Y15 (PACS) and X7 (RACS). Two possible origins for the short are:

1. Distortion of the flex leads by overheating due to excessive current
2. Distortion of the flex leads by gas bubbles inside the flex lead cavity

See my change

No history of excessive currents exists for these IRAs.

In a ground test, a short having resistance values within the range required to cause the flight offset was induced by injecting a bubble into the gyro flex lead cavity to force the flex leads against the gyro header. Changes in the bubble can be associated with motion and changes in temperature. The IRA 1009 anomaly occurred first and did not change with subsequent temperature changes; the amount of offset can be seen to vary during vehicle maneuvers. The IRA 1012 operated at a constant temperature until the RACS was turned off and then for a long period at a lower temperature before its anomaly appeared. On IRA 1012 the offset occurs after vehicle maneuvers and then disappears after a period of time (in the first occurrence it lasted from 1088 through 1101). The IRA 1012 offset was made to reoccur in SOLO Experiment ACS 200 by cooling for several revs (shut-down PACS) and then reheating. ? ?

The following tests have been implemented to detect similar problems on future IRAs:

1. Compare PACS and RACS channels using differential analyzers and recorders to detect small offset differences. This test also to be run at the launch base.
2. Tumble test to check for bubbles or any foreign matter in the gyros.

The following are being investigated as possible improvements:

1. Seal gyro bellows to offset altitude changes
2. Insulate the flex lead cavity and the gimbal snout by anodizing
3. Revise fill procedures to improve bubble and foreign matter exclusion.

2.1.6 PACS FCEA Failure

Following separation of RV-4, control of vehicle attitude was lost. The pitch rate following separation exceeded 5.6 deg/sec before the failure detector responded and closed Isolation Valve No. 4. Analysis showed that the FCEA pitch analog rate channel was not responding to sensed positive rates. Thus when a pitch-up maneuver was commanded, the thrusters remained full on during the period of the maneuver (approximately one minute on post-recovery pitch-up). Review of the data from earlier pitch maneuvers indicated that the failure occurred between Rev 940 and Rev 973. There was no loss of control during these earlier pitch maneuvers since they were negative (pitch-down) with an inertial return to horizontal. No positive (pitch-up) maneuver had been executed since RV-3 (Rev 715).

The cause of this anomaly has been diagnosed as an inoperative hybrid integrated circuit buffer switch on the rate processor subassembly in FCEA 1015. Corrective action has previously been implemented on the buffer switch to improve design reliability. The failure rate on this switch lot is not abnormal; therefore, no other corrective action is contemplated.

2.1.7 ACS Performance During Tumbling Capture (M1V2)

The pitch rate channel failure (FCEA) discussed in Section 2.1.6 resulted in the SV tumbling following RV-4 separation (Rev 1105.3). The tumble and subsequent capture occurred on the same system (M1V2). The significant tumble and capture times were as follows:

	Vehicle Time (sec)
RV 4 Sep	13947.0
FDU Enable	14037.0
FDU Closed IV 4	14074.6
ACS 2	14677.6
RCS IV 4 Open	14702.8
ACS 2 Exc	14707.8
H/S Search	14827.8
MCLR	19676.8

The failure detector (FDU) closed Isolation Valve 4 37.6 sec after the FDU enable. Although the pitch rate was in excess of 5.56 deg/sec prior to FDU enable, the SV rates at the time of IV 4 closing were as follows:

Pitch	2.02 deg/sec
Roll	0.03 deg/sec
Yaw	0.00 deg/sec

Following RV4 separation, the SV crossed the zero degree pitch attitude (nose forward) at 13962 sec vehicle time, and again (after one complete revolution) at 14188.6 sec vehicle time. This was observed using pitch H/S data.

Following initialization of the capture sequence (14707.8 sec vehicle time) the SV captured and was stable in the nose forward attitude on Rev 1106.2P at 18617 sec vehicle time, which was the first following real-time pass.

2.1.8 PACS Pitch Rate Noise

Bipolar noise spikes as great as 0.03 deg/sec peak-to-peak were observed on the PACS pitch rate output. The same type of noise spikes have occurred during module testing and noise of this magnitude would have been cause for removal of the IRA. At most, this noise may have caused some extra pulses on the RCS but was not sufficient to affect the system operation. The noise is attributed to components used in the gain change amplifier/demodulator area in the IRA pitch channel. Suspect components are being replaced.

2.2 REACTION CONTROL SYSTEM

2.2.1 Flight Summary

History of RCS propellant consumption is shown in Fig. 2-1 and the history of the flight is shown graphically in Fig. 2-2.

Satisfactory vehicle attitude and rate control were provided by the RCS at all times during the 91 day flight. Leaks developed in the primary system (RCS-1) as expected and control was switched to the standby system (RCS-2) on day 26. No leaks were detected in RCS-2 for the remainder of the flight and although some degradation of thrust was observed, the large degradation expected from ground tests did not occur.

2.2.2 Propellant Consumption

RCS propellant consumption for the 91 day mission was computed to be 870 pounds. Propellant was consumed from RCS-1 tanks 1 and 2 until day 26 when control was switched to RCS-2 which was fed directly from the main OAS tank as RCS tanks 3 and 4 were cut out of the system prior to flight. Abrupt temperature increases on both the REA and mount can be noted when the leaks began on RCS-1 and precede the onset of excessive propellant consumption. On RCS-2 no leak-significant increases in the mount temperatures (this is the only instrumentation available on RCS-2) and no significant increase in fuel consumption occurred.

2.2.3 Thruster Performance Degradation

The thrust level for each REA of RCS-1 was determined from the chamber pressure and temperature data. The thrust levels at the time of transfer to RCS-2 are shown in Table 2-1.

The REA thrust levels of RCS-2 were determined from the events listed in Table 2-2. Since ground test data indicated that a drop in steady state thrust would be the first indication of a failing thruster, a series of mini-pitch and mini-yaw maneuvers

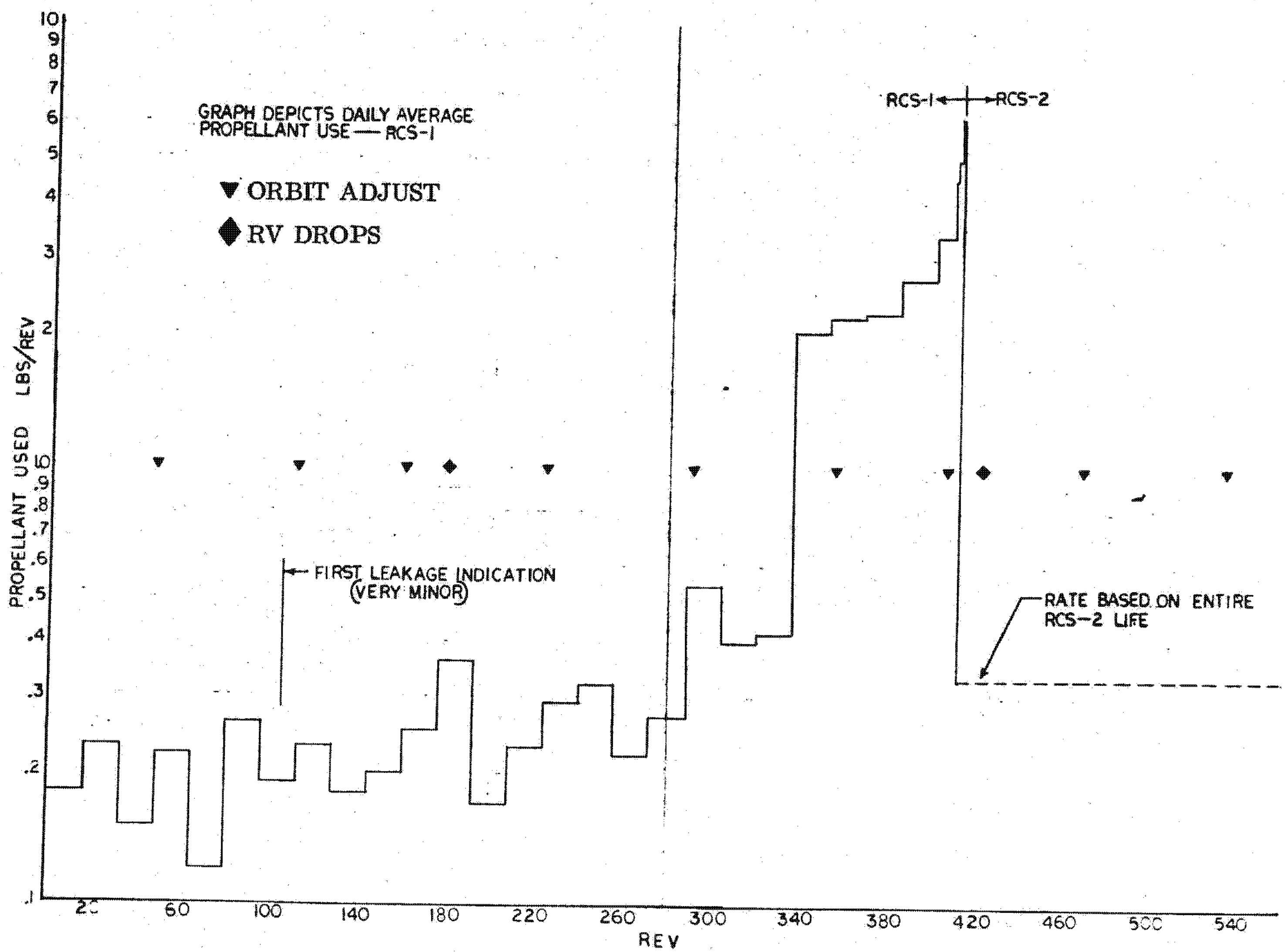

Fig. 2-1 RCS Propellant Consumption

BIF003W/2-068875-73

Page Denied

TABLE 2.1

RCS-1 THRUST AT TIME OF TRANSFER

Rev 406

Feed Pressure 160 PSIA

REA	P_C (PSIA)	Temp (^oF)	Thrust (lb)
1	63	612	3.3
2	62	1083	3.3
3	59	673	3.1
4	75	369	4.0
5	63	847	3.3
6	67	716	3.5
7	58	1058	3.0
8	75	933	4.0

P_C – Thrust chamber pressure in PSIA

Acceptance thrust level for thrusters at 160 PSIA is 3.8 to 4.4 pounds.

TABLE 2.2

BASIS FOR RCS-2 THRUSTER PERFORMANCE

A. Steady State Thrust

B. Average Valve "On" time per sec of Orbit Adjust Burn.

C. Average number of pulses per valve per second of Orbit Adjust Burn.

D. Average "Hot" Impulse bit.*

E. Average "Cold" Impulse bit**

F. Average Pulse Count per REA

*Hot impulse bit – the impulse bit generated by a REA that is at the equilibrium bed temperature for the frequency at which it is pulsing.

**Cold impulse bit – the impulse bit generated by a REA disregarding temperature.

producing steady state thrust were commanded and are noted on Fig. 2-2. Mini-pitch consisted of pitching the vehicle down 14^{o} and then flying for 3.5 minutes prior to reconnecting the Horizon Sensors which allowed the vehicle to reattain the proper flight attitude without additional commanding. The mini-yaw was a 14^{o} yaw and then a commanded return to the zero yaw position. Results obtained are shown in Fig. 2-3, and Fig. 2-4. Figure 2-3 is a non-normalized plot and shows the method of determining the thrust is accurate enough to follow the normal blow down curve. Figure 2-4 presents the REA thrusts normalized to a 220 psi feed pressure plotted against pulse count. Included on Fig. 2-4 are the results of the combined system ground test at Rocket Research. The thrust degradation at 60-70,000 pulses seen in the ground test did not materialize in flight. It can be seen that only one thruster significantly exceeded the ground test pulse life; however, the more important parameter, mission days, was more than doubled.

On SV-5, there will be a better opportunity to evaluate the long term thruster performance as thrust chamber pressure and temperature will be available for thrust determination since RCS-1 will feed directly from the OAS tank and will be the long term control system.

2.2.4 Conclusions

- Elimination of the present RCS tankage using EPT10 rubber diaphragms stops the gross valve leakage problem experienced on previous flights
- Thrust degradation was not accelerated by operation at duty cycles (and temperatures) lower than the Rocket Research ground test. The degradation observed in operation on the ground was not confirmed in orbit operation.

30

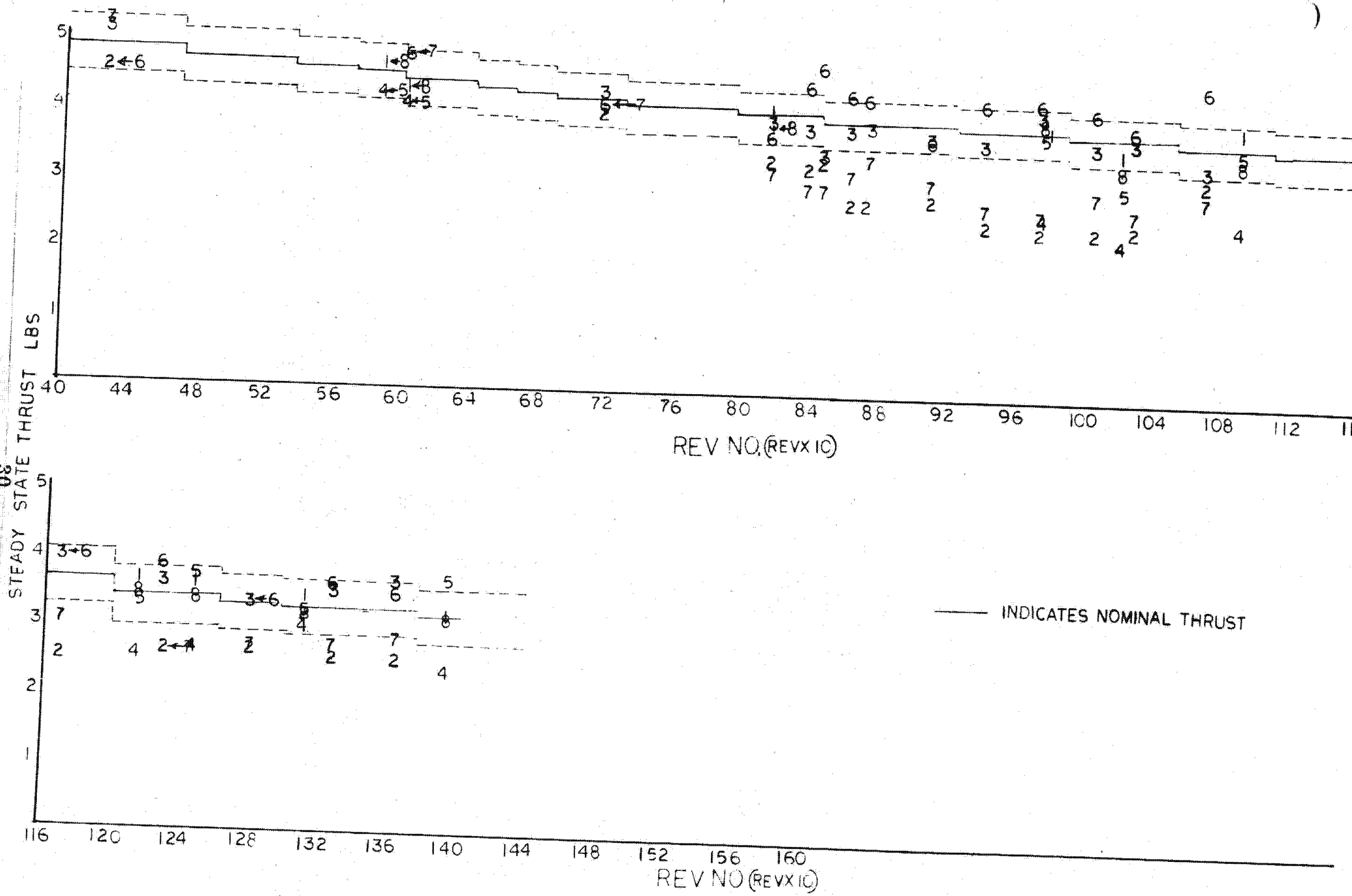

Fig. 2.3 Steady State Thrust Trends

BIF003W/2-068875-73

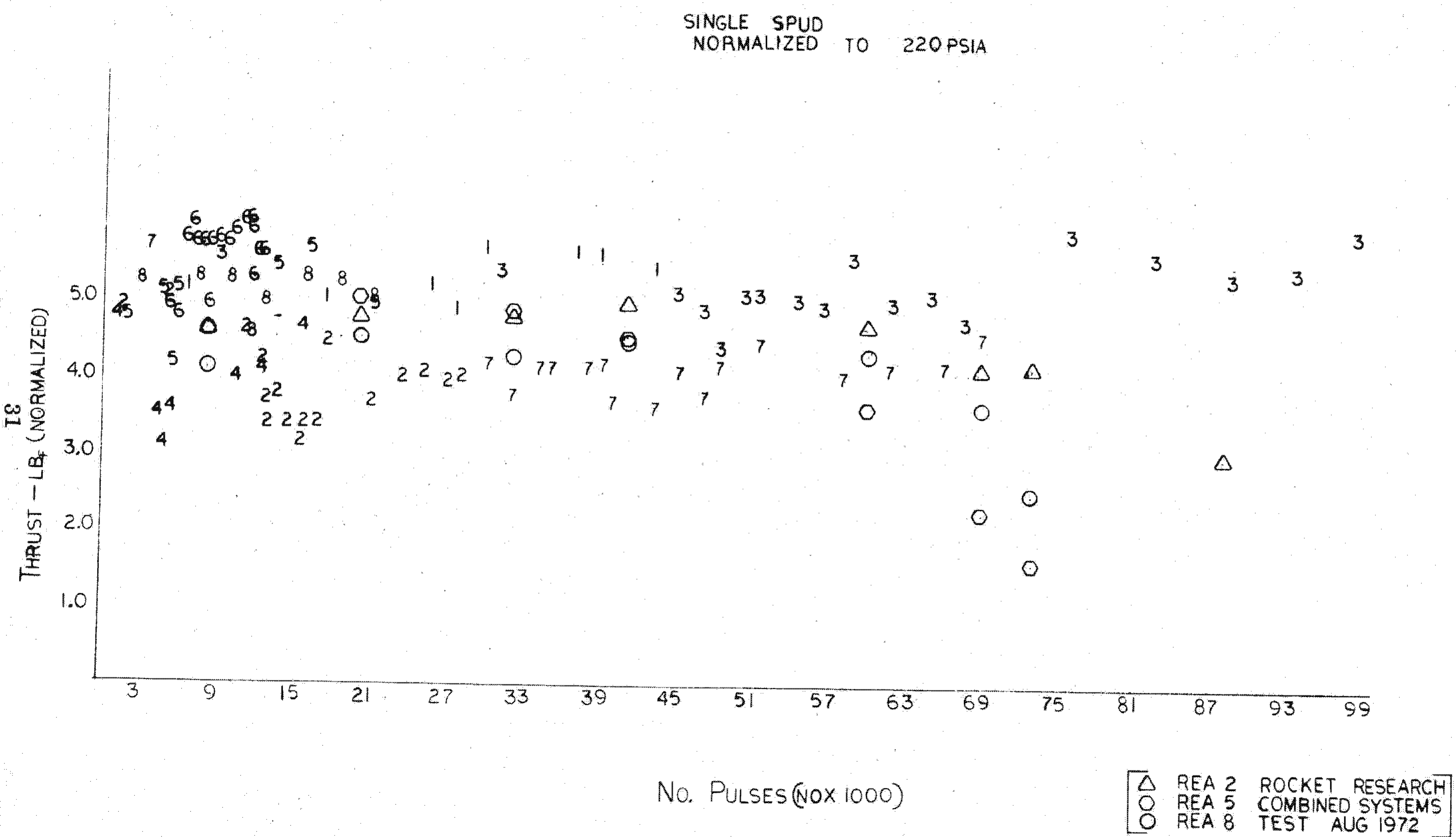

Fig. 2-4 RCS Thruster Health

31

BIF003W/2-068875-73

Section 3
ORBIT ADJUST

3.1 ORBIT CONTROL

The Orbit Adjust System was utilized eighteen times during the active mission for drag makeup, perigee location control and ground trace control. The OA firings were all normal and the engine performance was well within specifications.

The OAS was utilized six times during the SOLO phase of the mission for drag make-up. Three additional firings were used to place the vehicle in an orbit with a 65 nm perigee for four revs before deboost.

System performance is summarized in Table 3-1.

3.2 DEBOOST

The final firing of the OA engine was for the deboost on Rev 1463. The firing duration was 486.2 seconds to achieve a planned negative velocity increment of 222 ft/sec.

Table 3-1

OAS PERFORMANCE

OA Firing No.	Rev Number	Impulse Delivered (lb-sec)	Planned ΔV (ft/sec)	Achieved ΔV* (ft/sec)	Percent Error in ΔV
1	47	9424	15.57	15.56	-0.06
2	111	17623	29.00	29.14	0.48
3	160	13904	22.97	23.14	0.74
4	225	21498	39.23	39.16	-0.19
5	290	20422	37.42	37.42	0
6	355	17603	32.25	32.43	0.55
7	406	16233	30.10	30.06	-0.13
8	468	18896	38.97	39.04	0.18
9	533	12280	25,35	25.50	0.59
10	598	23516	48.86	49.08	0.45
11	600	6499	-13.68	-13.62	-0.46
12	663	17796	37.23	37.36	0.35
13	728	13810	32.46	32.51	0.15
14	792	14820	35.16	35.05	-0.32
15	857	15096	35.86	35.90	0.11
16	922	9641	22.86	23.03	0.74
17	987	12462	29.76	29.91	0.50
18	1052	13418	32.36	32.37	0.03
19	1109	10020	24.54	24.35	-0.82
20	1158	9849	27.00	27.11	0.41
21	1199	14491	40.44	40.71	0.69
22	1264	7904	22.50	22.40	-0.44
23	1297	11047	31.42	31.42	0
24	1378	10874	31.24	31.13	-0.35
25	1457	19202	55.26	55.38	0.22
26	1458	17744	51.24	51.54	0.58
27	1459	15218	-44.45	-44.49	0.09
DeBoost	1463	75549	-222.19	-	-

*Determined from the tracking ephemeris data.

Section 4

TRACKING, TELEMETRY AND COMMAND

4.1 TRACKING

4.1.1 Accuracy

An evaluation of tracking accuracy is being prepared by the FTFD and will be available through that office.

4.2 TELEMETRY

4.2.1 General Performance

Telemetry system performance was satisfactory throughout the flight.

4.2.1.1 Usage Summary Through Revolution 1463

SGLS	Side 1	Side 2
• Number of ON/OFF cycles	1404	145
• Operational Time (min)	8899	1228
TM		
• Total Operational Time (min)	20,310	6323
• Number of ON/OFF cycles	8183	2938
Tape Recorder	**No. 1**	**No. 2**
• Number of ON/OFF cycles Record	8708	865
• Record Time (min)	15,966	1036
• Reproduce Time (min)	2984	215
• ON/OFF cycles Reproduce	1024	78

4.2.2 Delayed Acquisition on High Elevation Passes

SV-4 experienced delayed acquisition on high elevation passes predominately during passes with a maximum elevation of $38^{\circ} \pm 10^{\circ}$ and on the left side of the vehicle. A comparison of output power, modulation loss on the SGLS subcarriers, and antenna patterns taken from SV-3 and SV-4 flight data shows the only differences between SV-3 and SV-4 are: (1) SV-4 was 0.5 db lower in output power than SV-3, and (2) a modulation index analysis shows the modulation loss on SV-4 is 0.6 db greater than SV-3. This accounts for a total of 1.1 db difference. This difference could account for a delayed acquision of up to 3°.

For SV-5 the modulation indexes have been adjusted to reduce the 1.024 MHz SCO modulation loss. This adjustment will increase the downlink real time performance by several db.

4.2.3 Instrumentation

The following comprises the list of anomalous instrumentation existing at liftoff.

ID No.	Description	Status
H012	PCM #1 Bit Rate Indicator	Can Indicate 128 KB instead of 48 KB
Z529	MS Temp Monitor	Invalid Readings

4.3 COMMAND

4.3.1 Uplink Operation

The vehicle SGLS command equipment was utilized to receive approximately 11.2 million bits with no vehicle problem indications.

4.3.2 GFE Command System

4.3.2.1 Extended Command System. The ECS responded satisfactorily in all command modes resulting in the loading of 139, 367 SPC's in memory; of these 139,367 SPC's loaded, 78,081 were output by both PMU's for decoder processing. The remainder were erased prior to their time label matches.

4.3.2.1.1 ECS Clock Operation. The accuracy of the clock throughout flight has been determined to be 0.23 parts in 10^6. The clock oscillator frequency changed 0.12 Hz in 91 days.

4.3.2.2 Minimal Command Subsystem. The MCS responded correctly to all commanding.

4.3.2.3 Remote Decoder/Backup Decoder. Both sides of the Remote Decoder were utilized for each of the four recoveries. Performance of both sides was determined to be acceptable through analysis of telemetry data.

4.3.2.4 Command System Usage Summary Through Rev 1463.

System	Total Operating Time (hours)
ECS	2195
MCS	6
Remote Decoder	4.5
Backup Decoder	3.5

4.3.3 375 MHz Receiver

The 375 MHz Receiver was powered during the entire mission with no anomalies.

4.3.4 Data Interface Unit

The data interface unit performed satisfactorily throughout the flight.

Section 5
ELECTRICAL DISTRIBUTION AND POWER

5.1 SOLAR ARRAYS

Solar Arrays were extended on Rev 1. The left array started deployment on command and required 640 seconds to complete deployment and erection. The right array did not start to deploy until 1680 seconds after receiving the command and then required approximately 750 seconds to complete deployment and erection. Power output from each leg exceeded the specification value. Degradation from the initial output to end of the fourth segment was 2 percent. 2 percent is well below the 5 percent allocated.

5.2 MAIN BUS VOLTAGE

The Main Bus voltage varied from a low of 27.0 to a high of 31.8 volts. The allowable range was 25.5 to 33.0 volts. Low voltage data was obtained in the dark with a bus load of 70 amps. High voltage data was gathered during charge cycles.

5.3 POWER CAPABILITY AND USAGE

Power usage ranged from 217 to 352 amp-hours/day. This is well below the 400 amp-hour/day capability. Excess capacity was demonstrated by K2 charge relay cutoffs occurring on Rev 7 and essentially every rev thereafter except those with heavy payload operations.

5.4 TYPE 29 BATTERY PERFORMANCE

All Type 29 batteries operated in a desirable environment (42^{o}F to 51^{o}F) and performed normally throughout the mission.

5.5 PYRO BATTERY PERFORMANCE

Pyro Battery 1 stabilized at 49°F thus minimizing self discharge during the events. Twenty-three days after launch the battery left the peroxide region indicating a computed 3 amp-hours had been removed leaving 10 amp-hours for continued use. After seventy days calculated capacity was 6.3 amp-hours. Cell degradation life still available was 46 days. Pyro Battery 2 followed the same pattern with the exception of leaving the peroxide operating region on Day 18.

5.6 LIFEBOAT BATTERY PERFORMANCE

The Lifeboat Battery operated normally in a 49°F environment throughout the entire mission. A total of 97 amp-hours remained at the end of the fourth segment from an initial 354 amp-hours at launch. Remaining cell degradation life was 56 days.

Section 6
LIFEBOAT II

6.1 HEALTH CHECKS

The Lifeboat data that was examined is summarized in Table 6-1. The magnetometer sensor data indicates equivalent attitude errors as follows:

Magnetometer	Attitude Error
Q	-0.9 to +0.2 degrees
P	-0.5 to +0.2 degrees
R	-0.3 to +1.0 degrees

The rates measured on the three Lifeboat II rate gyros were within 0.10 degrees/sec of the rates measured on the ACS gyros.

6.2 INERTIAL RV RECOVERY EXPERIMENT

The vehicle was inertially flown so as to be in an RV recovery attitude with a pitchdown of -40.7 degrees at KOD1 at System Time 75785.6 on Rev 813. Based on the observed position of the vehicle after the ACS programmed pitchup, the actual pitchdown at separation was 0.22 degrees greater than desired.

DGMAP using the inertial stabilization option was used to predict the theoretical P, Q and R magnetometer readings to be expected at POGO and KODI for the predicted inertial position of the vehicle. The predicted and observed sensor readings and the predicted and observed pitch angles are shown in Fig. 6-1. It can be seen that the R sensor reading at POGO established the attitude to be about one degree less than the true position of the vehicle if the 0.22 degree error is added to the difference on the graph. The P sensor is above the saturation level of the TM at POGO. At KODI the R sensor saturates the TM but the P sensor established the pitch attitude to be about 0.4 degrees less than the actual.

The Q sensor (sensing yaw) was within 3 milligauss of the predicted values from DGMAP which is equivalent to an error of about 0.33 degrees (these values were not plotted). These values are well within the ±3 degree tolerance on attitude for RV ejection and will provide a reliable check on the position if inertial flight is used for a recovery.

6.3 FUNCTIONAL HEALTH CHECK

To ensure that the Lifeboat II system could perform a deboost if required, a functional health check was conducted on Rev 1210.

The ACS thruster power was removed and Lifeboat II was allowed to control the vehicle for 30 seconds.

The Lifeboat II performed as expected, pitching down approximately 20 degrees and yawing approximately 14 degrees before being reset.

TOP SECRET / H

Table 6-1

LIFEBOAT II OPERATION

Rev	Mode	Q Magnetometer (Milligauss)		R Magnetometer (Milligauss)		P Magnetometer (Milligauss)		Y Axis Gyro (deg/sec)	
		Observed	Theoretical	Observed	Theoretical	Observed	Theoretical	Observed	Theoretical
18.4	SN-DB	-23	-19.9	Saturated	Saturated	Not in use	-	-0.05	-0.069
		-23	-20	206	208.6	Not in use	-		
	SN-RV	-29	-21.2	Not in use	-	Neg. Sat	Neg. Sat		
		-26	-19.9	Not in use	-	Neg. Sat	Neg. Sat		
		-23	-19.8	Not in use	-	Neg. Sat	Neg. Sat		
	NS-RV	-23	-21.2	Not in use	-	Neg. Sat	Neg. Sat		
180.3	NS-RV	-26	-24.7	Not in use	-	Saturated	Saturated		
	NS-DB	-29	-24.7	Saturated	Saturated	Not in use	-	2.11	2.15
	NS-RV	-29	-26.8	Not in use	-	221	215.2	0.27	0.227
423.3	NS-DB	-38	-35	Saturated	Saturated	Not in use	-		
	NS-RV	-38	-35.4	Not in use	-	218	224	2.28	2.31
	NS-RV	-38	-36.4	Not in use	-	218	222.3		
715.3	NS-DB	-38	-34.4	Saturated	Saturated	Not in use	-		
	NS-RV	-38	-35.2	Not in use	-	218	216	2.37	2.39
1105.3	NS-DB	-20	-17.1	Saturated	Saturated	Not in use	-		
	NS-RV	-20	-17.4	Not in use	-	221	225	3.07	3.10
1210.2								X Axis Gyro	
								0.13	0.04
								0.06	0.07
								Z Axis Gyro	
								0.39	0.48
								0.62	0.61

TOP SECRET / H

BIF003W/2-068875-73

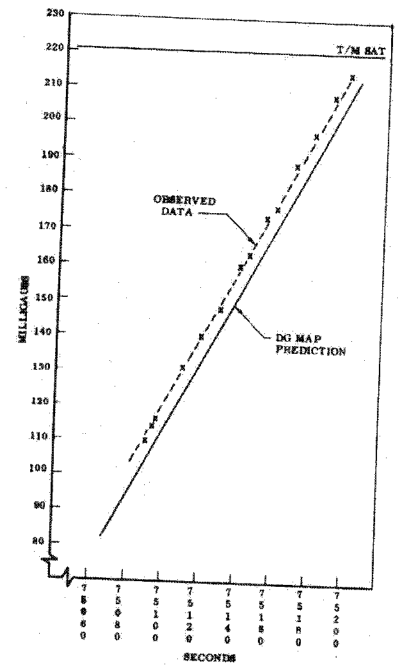

Fig. 6-1a

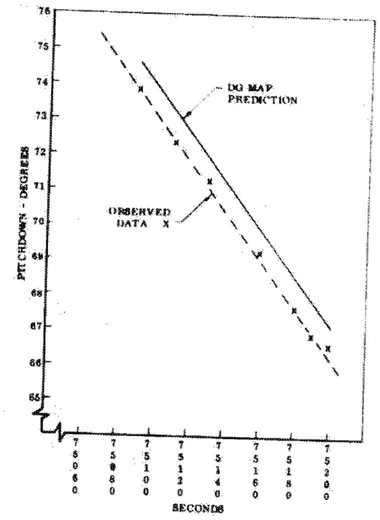

Fig. 6-1b

R Sensor in N-S RV Recovery Mode Over POGO (P Sensor Saturates TM)

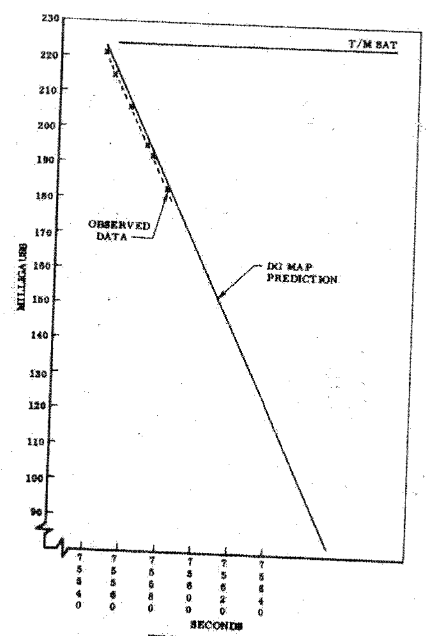

Fig. 6-1c

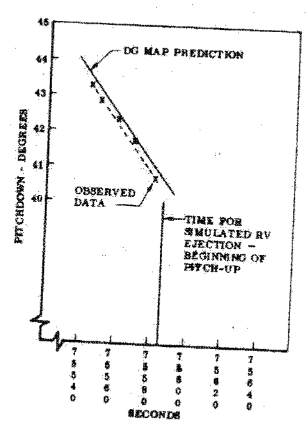

Fig. 6-1d

P Sensor in S-N Deboost Mode Over KODI (R Sensor Saturates TM)

Fig. 6.1 Vehicle Attitude as Determined by Lifeboat II During Inertial RV Recovery Experiment (Rev 813)

Section 7

SENSOR SYSTEM

7.1 COARSE FILM PATH

Both coarse film paths – supply, loopers, steerers, articulators and takeups – exhibited nominal operation throughout the mission with the following exceptions.

- On Rev 474 in RV-3, an ESD occurred on the A side (forward looking) camera after the sixth frame of a planned 43 frame operation at which time the looper carriage contacted the travel limit switch. Flight data indicated a fine film path hang-up with the metering and drive capstans acting erratically from start-up until the ESD. Post flight inspection of the film showed markings and degraded imagery which confirmed the probable cause as being drag of a roller or capstan near the input of the fine film drive. At this ESD shutdown, the looper and fine film tension 5 returned to normal and recovery from this anomaly was completed successfully with normal operations resuming on Rev 508.

- Post-flight inspection of the RV-3 A side film revealed a film tear occurring during operation on Rev 640. Markings indicated that the tear occurred while the film was moving forward after exposure but analysis of the film path diagnostic data showed no discernable disturbance associated with the tear.

- On Rev 1101 in RV-3, an ESD again occurred on the A side camera during the first of two engineering MOP's. Flight data indicated that the supply had been depleted and subsequent operations with the ESD disabled confirmed this as the cause of the ESD and also assured that the end of the A side film was spooled on the take-up.

During the mission the basic constraints on rewind and scan center were modified as follows:

- Starting on Rev 508 all operations were terminated with a 5 inch per second rewind. Nominal operation was exhibited.
- On Rev 898, commencing the start of stereo operation with color film in the A-side camera, the scan center was constrained to zero degree. This constraint was relaxed to zero and ±15 degree scan centers on Rev 930 and subsequently relaxed to the basic constraint of zero, ±15 and ±30 degree scan centers on Rev 960. As in the case of the rewind constraint relaxation, coarse film path operation remained nominal.

7.2 FINE FILM PATH

Both fine film paths exhibited nominal operation throughout the mission with the exception of the A side camera hang up on Rev 474 in RV-3 which resulted in excessive looper travel and subsequent ESD as described in paragraph 7.1.

7.3 COMMAND AND CONTROL

The command and control subsystem exhibited nominal operation throughout the mission in both stereo and mono modes with the following exceptions.

- A failure of an A-side camera interlock source signal on Rev 778 in RV-4 necessitated disabling of verification circuitry to complete the mission.
- Early in RV-1, improper stowing of the optical bars was observed on some operations due to camera power being removed before the optical bars had stowed. This occurred because optical bar shut-down time resulting from a BUFT - (Backup Film Transport Minus) command, which was being used to meet the zero rewind constraint, can be longer than that for a normal shut-down command due to uncertainties of optical bar position during BUFT - shut-down. Further occurrences were precluded by adding an additional 13 seconds to the optical bar shut-down time calculated by the software for normal shut-down.

All ESD's experienced were attributed to coarse and fine film path anomalies discussed in paragraphs 7.1 and 7.2.

Following the development of an SV attitude error on Rev 1088 in RV-4, the command system was used to bias Vy and O^2A^2 (On-Orbit Attitude Adjust) values in an attempt to correct for this error. Five stereo and three mono B side operations were run with this bias but just prior to the last operation (in mono B side) the SV attitude error disappeared with the result being incorrect Vy and O^2A^2 values for this operation.

7.4 OPTICAL BAR PERFORMANCE

The optical bar performance of both cameras was nominal throughout the mission with the exception of the improper stowing early in RV-1 as discussed in paragraph 7.3. Subsequent analysis and in-flight experiments showed a large change of corrector plate temperature resulted from this condition which would significantly degrade photography. Operations 12 and 32 cited as of very poor quality followed improper stowing.

7.5 INSTRUMENTATION

All instrumentation, other than the A-side camera interlock source which failed on Rev 778 in RV-4, was operative throughout the mission.

7.6 PNEUMATICS

Pneumatics system performance was nominal throughout the mission. Gas usage was 31.7 pounds with 2.3 pounds remaining.

Section 8
REENTRY VEHICLES

8.1 SUMMARY

The recovery statistics are shown in Table 8-1 and Fig. 8-1. Performance of the RV Subsystems is summarized in Table 8-2. Data indicate that all RV events (on-orbit, re-entry and recovery) occurred as planned (except for delayed separation of the propulsion truss on RV-2) and the RV flights followed the predicted trajectories. The delayed truss separation had no subsequent effect on the flight.

The payloads on RV-1 and RV-2 were recovered in good condition. On RV-3 and RV-4 the fragments of an epoxy protective cover from a relay panel in RV-4 were found within the wraps and within RV-3 and RV-4. After the recovery of RV-4 the battery case failed, contaminating the loose outer wraps of the stock. The outer wraps were loose on RV-1, RV-2 and RV-4 due to payload rotation after aerial retrieval induced shearing of the core pins. Aerial retrieval loads exceeding the core pin strength were anticipated.

All subsystems performed satisfactorily and met all mission requirements as shown in Table 8-2.

8.2 REENTRY VEHICLE PERFORMANCE

All RV on-orbit functions were normal and occurred on time. The SV provided a satisfactory pitch angle for each RV separation. All other SV/RV interface functions were nominal.

The RVs were adequately spin stabilized during the exoatmospheric coast and retrograde phase of the reentry trajectory. Figure 8-1 shows the entry conditions to be well within previously established entry boundaries. Also shown are the conditions at time of drogue chute deployment which are within the design envelope.

Table 8-1

RV RECOVERY SUMMARY

	RV-1	RV-2	RV-3	RV-4
RV Serial No.	20	19	18	17
Recovery Rev No.	180	423	715	1105
Recovery Date (1972)	21 Oct 1972	5 Nov 1972	23 Nov 1972	17 Dec 1972
Payload Weight (lb) (A; B) (Measured Wt from Recovered RV)	A = 223.1 B = 224.8	A = 229.0 B = 229.0	A = 211.5 B = 216.5	A = 213.3 B = 203.7
Unbalance Percent	0.7	0.0	2.2	3.9
SV Orbit (hp x ha/ωp)*	89.2 x 148.6/145.9	87.9 x 157.3/131.6	90.9 x 145.2/132.2	91.7 x 144.7/119.6
SV Pitch Angle (deg)	-37.9	-41.0	-41.8	-41.5
Nominal PIP Latitude	24.5°N	18.0°N	18.0°N	23.5°N
Impact Location Error (EPPD vs Teapot Eval)				
Overshoot (nm)	0.1	10.4	7.0	2.0
Cross Track (nm)	1.2E	3.0W	2.8E	3.9W
Recovery (Aerial)				
Altitude (ft)	12,500	6,800	10,500	11,000
Parachute Condition	No Damage	No Damage	Minor Damage	No Damage
Retrieval Pass	1	3	1	2
RC/Payload Condition	Good	Good	Good	RC Condition Good Approx 330 feet of Payload Damaged by Battery Electrolyte

*hp = Altitude of Perigee (nm), ha = Altitude of Apogee (nm), ωp = Arg of Perigee (deg)

BIF003W/2-068875-73

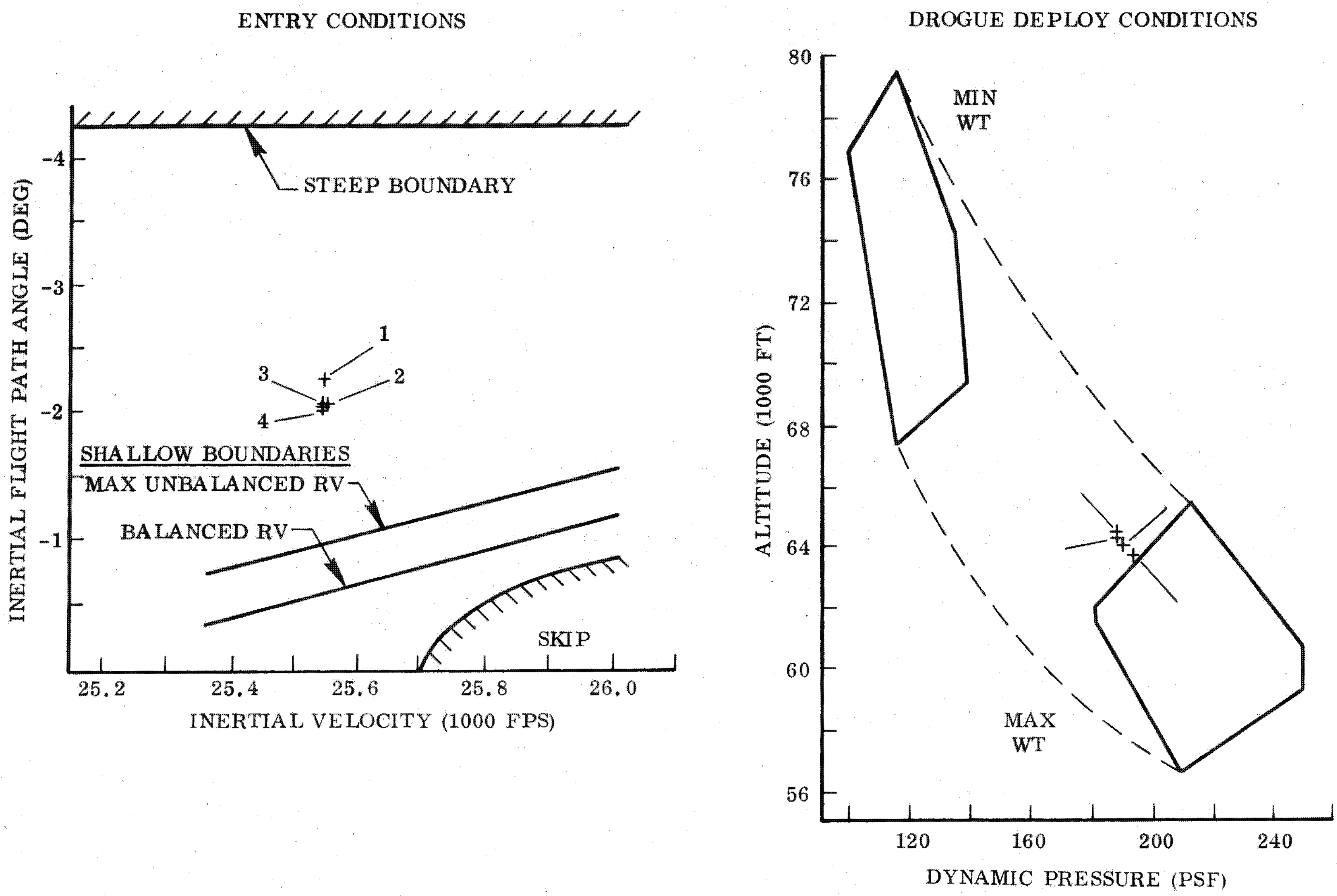

Fig. 8-1 SV-4 Reentry Parameter Comparisons

BIF003W/2-068875-73

Table 8-2

RV SUBSYSTEM PERFORMANCE SUMMARY

RV Subsystem/Function	Performance Assessment
On-Orbit Thermal Protection	Normal • T_{PL} Container = T_{ref} $^{+2^{\circ}F}_{-5^{\circ}F}$ • Power Usage (Watts/RV) Maximum = 18 (First Day in Orbit) Stabilized = 6 (Sixth Day in Orbit) Allowable = 20
Trim and Seal	Normal
Electrical Power & Distribution	Normal during life of mission • All Batteries Activated • All Voltages 27.2 Volts • RV 2 Pyro Battery 2 leaked electrolyte • RV 4 Pyro Battery 2 had a seam rupture occurred onboard retrieval aircraft
Sequential Subsystem	Normal on RV-1, RV-3 and RV-4 • TM and postflight test verified RV 2 primary and redundant systems functioned properly for retro truss separation. Inspection indicates physical separation did not occur properly.
Pyro Subsystems	Normal • All primary and redundant pyrotechnics in each RV were verified by post flight inspection to have functioned properly.
Spin Stablilization	Normal
Retro Motor	Normal
Tracking, Telemetry, Instrumentation	Normal
Heat Shield	Normal
Base Thermal Protection	Normal
Structure	Normal
Recovery System	Normal • Heavy suspension lines were broken during tow period on RV-1 and RV-2

8.3 REENTRY VEHICLE SUBSYSTEM PERFORMANCE

Review of the Reentry Vehicle subsystems indicates four anomalous conditions.

- Delayed retro truss separation on RV-2
- Relay panel epoxy cover failure on RV-4
- Pyro battery case failure on RV-2 and RV-4
- Heavy load lines on main parachute broken on RV-1 and RV-2.

Fragments of the truss assembly on RV-2 provided positive evidence that truss separation did not occur normally even though the attaching bolts were fractured at the proper time. Available evidence indicates that the pyro system fractured all bolts but that friction or interference of the separating elements delayed separation. Truss attachment details have been redesigned to eliminate the shear pins and provide bolts with controlled separation planes. This redesign, which precludes recurrence of this anomaly, will be flown on all future flight vehicles.

A protective epoxy cover on the back of the RV-4 Power and Control Relay panel fractured during orbital operations. Fragments of the epoxy were transported through the film path into RV-3 and pieces were found wrapped within the stacks and lying loose within both vehicles. Post flight dissection of the panel revealed that the epoxy was thinner than normal and that the panel filler material had a spongy texture near wire bundles. Exact cause of failure is being investigated. Pending a final determination of the failure and final design configuration, an interim fix, consisting of taping the epoxy on all relay panels, will be used to preclude escape of loose epoxy in the event of a fracture.

Pressure buildup caused case failures of pyro batteries in RV-2 and RV-4. The failure on on RV-2 was typical for a battery with a blocked vent. Leakage of gas products and some electrolyte occurred at the electrical connector seal at the case wall. On RV-4, the pressure buildup appears to have been of an explosive nature, causing the metal case to rupture. Failure analysis has not been completed to date. In the interim, redesigned internal vents have been included in all future flight vehicle batteries (both pyro and main). This will eliminate pressure buildup and minimize the probability of case failure. Analyses are continuing to determine the cause of the explosive failure.

Chute behavior was essentially similar to that observed on prior flights except for the heavy suspension lines. During the aerial retrieval one of the eight heavy suspension lines was broken on RV-1 and three were broken on RV-2. The breaks are the result of abrasive action of other slack members during the tow period prior to boarding. This phenomena is self limiting in that as lines are broken fewer slack members are present to cause abrasion. There will always be a sufficient number of active lines (strength) to successfully board the RC. Operational procedures, such as, minimum tow time, aircraft velocity and mild aircraft maneuvers are emphasized to minimize the damage due to abrasive action.

(b)(1)
(b)(3)

Page Denied

Section 10
SUBSATELLITE

10.1 SUBSATELLITE PERFORMANCE SUMMARY

A 149 lb subsatellite system mounted on the +Y side of the SV forward section was carried into orbit. The separation sequence was in the pad load. The subsatellite was separated on Rev 2 at 13° South latitude on the ascending node. All subsatellite separation events were within desired tolerances and a nominal orbit was achieved by the subsatellite.

Section 11
STELLAR-TERRAIN SUBSYSTEM

There was no Stellar-Terrain Subsystem flown on SV-4.

Section 12
THERMAL CONTROL

12.1 FORWARD AND MID SECTIONS

The Forward and Mid Section structural temperature control is summarized in Table 12-1. The data indicates that the Forward and Mid Section thermal design provides good control of payload temperature levels. No design changes are forthcoming as a result of flight performance.

Table 12-1
FORWARD AND MID SECTION TEMPERATURES FOLLOWING INITIAL TRANSIENT

Parameter	Design Limits (^{o}F)	SV-4 Actuals
T_{FWD}	47/93	80/83
$\bar{T}_{TCA}$	48/92	74/76
$\bar{T}_{FWD} - \bar{T}_{TCA}$	< 20	5/7
T_{SU}	49/91	76/78
$\bar{T}_{SU} - \bar{T}_{TCA}$	6/-4	1/2

Definitions:

T_{FWD} – Average radiation temperature of the Forward Section derived from the average bulkhead temperature

$\bar{T}_{TCA}$ – Average radiation temperature of the forward compartment structure in the Mid Section

$\bar{T}_{SU}$ – Average radiation temperature of the aft compartment structure in the Mid Section

This flight utilized redesigned flight calorimeters on the forward and mid sections. The intent of the redesign was to reduce the error introduced by communication of the calorimeter with the surface to which it is mounted. A comparison of the maximum and minimum temperatures measured by the sensors on the SV-3 and SV-4 flights is shown below.

		Min/Max Temperatures (°F)	
Sensor	Location	SV-3	SV-4
A431	M/S +Y	-107/10	-97/13
A432	M/S +Z	-35/124	-34/130
A433	M/S -Y	-80/173	-95/190
A434	M/S +X	-60/94	-33/103
A458	M/S +Y	-100/-22	-91/-30
A459	M/S +Z	-55/55	-34/50
A460	M/S -Y	-82/85	-88/60
A600	F/S 1642 Bulkhead	-105/229	-100/220

The effect of the redesign is most apparent in the case of a white calorimeter (A460). This calorimeter is mounted on a black multilayer blanket with a temperature similar to that measured on A433, a black calorimeter. The blanket was somewhat hotter on SV-4 than on SV-3 as shown by A433 but A460 indicates an average temperature drop of 15°F and maximum temperature decrease of 25°F on SV-4 indicating the communication between the calorimeter and the blanket surface has been decreased by the redesign.

12.2 ACTIVE THERMAL CONTROL

The Active Thermal Control System performed normally throughout the primary mission. T_{REF} which represents the average Mid Section film path temperature was usually between 73°F and 75°F.

The RV heater zones which are actively controlled relative to T_{REF} were generally within 1°F of T_{REF} indicating adequate performance of the Active Thermal Control System.

12.3 AFT SECTION

Acceptable Aft Section temperature control was maintained throughout the flight. All equipment temperatures remained within design temperature as indicated by the temperature summary in Table 12-2.

Equipment and structure temperatures indicated contamination degradation to external vehicle thermal control surfaces similar to that noted on all other flights. The amount of degradation appears to be less than occurred on SV-1, about the same as SV-2, and greater than occurred on SV-3. The amount of degradation was within the bounds of preflight analysis, as is indicated by Figure 12-1, which compares actual door temperatures with the pre-flight predictions.

To provide capability for dual ACS operation on SV-4, a paint pattern change was made to the Bay 7 door and heat straps were added between the ARM and the Bay 6 door. It is estimated that these changes decreased IRA operating temperatures by approximately 30°F, resulting in satisfactory IRA temperatures during dual operation. Flight data indicates that the heat strap design performed as predicted based upon pre-flight analysis.

Table 12-2

SV-4 AFT SECTION CRITICAL COMPONENT TEMPERATURES

Critical Component	Design Limits (^{o}F)	SV-4 Actuals (^{o}F)(2)
	EDAP	
PDJB	-30/170	58/61
CCC's	-30/170	82/94
Batteries, Bay 3	35/70	41/45
Batteries, Bay 1	35/70	45/50
PDA's	-30/160	81/100
Solar Arrays	-125/225	-72/162
	ACS	
IRA	50/130	93/113
HSA Heads	0/130	64/86
FCEA	-30/160	93/107
	OAS	
Tank	65/100	79/91
Quad Valve	35/200	113/122(1)
Catalyst Bed	---	125/155(1)
	T&T	
Tape Recorders	20/130	80/102
Transmitters	-30/170	80/103
PCM Master	-30/170	94/115
PCM Remote, Bay 2	-30/170	54/64
PCM Remote, Bay 10	-30/170	107/114
	Command	
PMU A	-40/145	98/101
PMU B	-40/145	111/114
Clock	-40/153	113/115
MCS	-40/149	98/103
	RCS	
Tanks	40/140	72/104
Plumbing, Bay 12	35/140	81/94

(1) OA not firing
(2) Steady-state

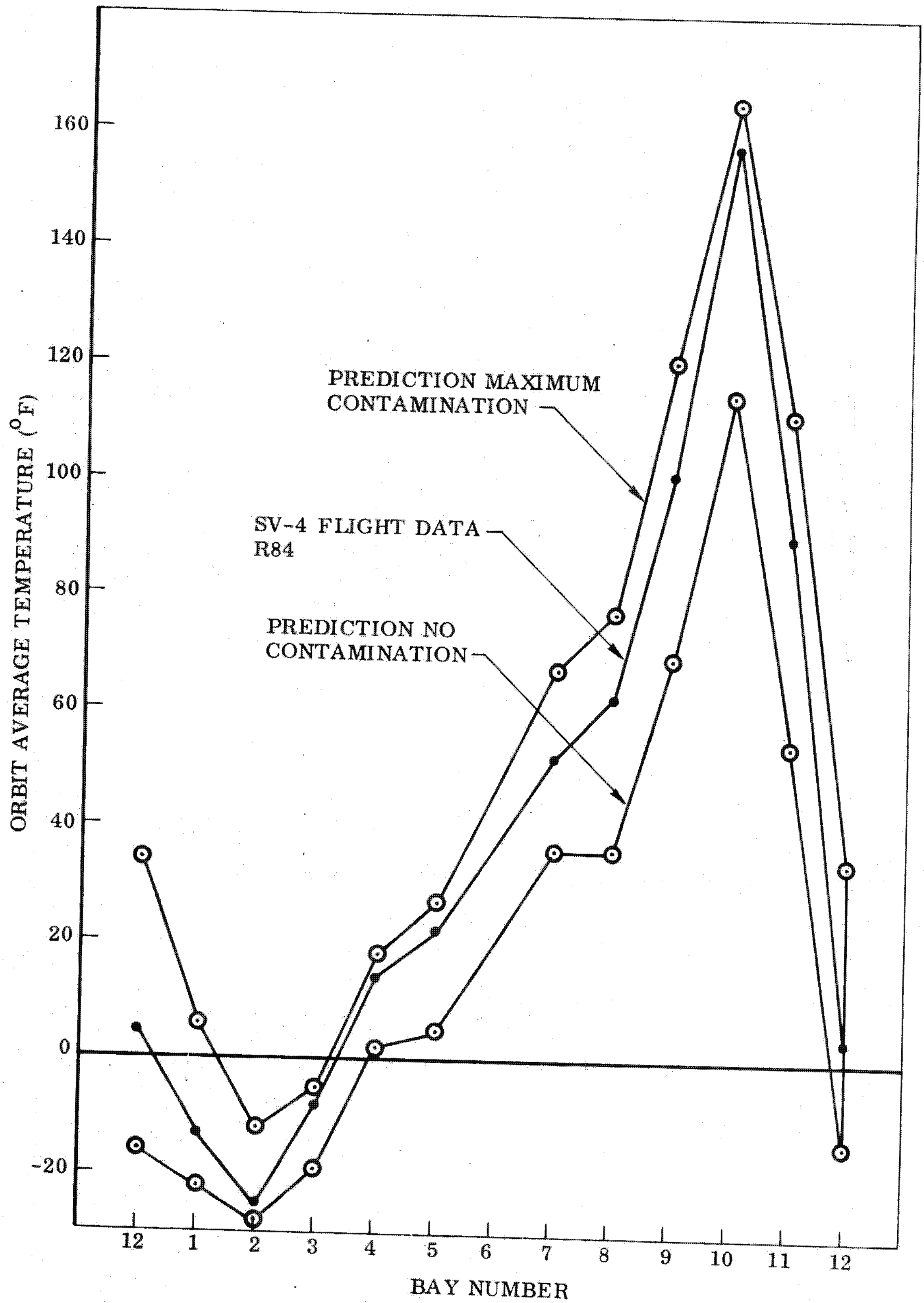

Fig. 12-1 SV-4 Equipment Door Temperatures

12.4 CONTAMINATION EXPERIMENTS

12.4.1 Description

Additional contamination experiments were flown on SV-4 to measure two distinct contamination environments. The first group of experiments, installed on Bay 12 of the Aft Section as shown in Fig. 12-1, were designed to measure the ascent contamination in terms of mass deposit and the effect of this mass deposit on the surface properties of FOSR (Flexible Optical Solar Reflector). Note that the blow-off shield was not used as on SV-2 and SV-3 to isolate the effects of the ground lift-off cloud. Note also that the QCM's (Quartz Crystal Microbalances) have a mass rate channel added for this flight as was done for SV-3 to help interpret the readings of the mass channel. The second set of experiments were installed on the aft bulkhead at Station 2203 as shown in Fig. 12-2. These devices were designed to monitor the mass deposit produced by the RV retro motors and to assess the effect of the mass deposit on the surface properties of white silicone paint and FOSR.

12.4.2 Results

12.4.2.1 Aft Section — Bay 12. Orbital temperature data indicated the following apparent solar absorptivity (α) value:

Surface	Preflight α	Orbital Data α	$\Delta\alpha$
White paint Bay 8	.22	.54	.32
White paint Bay 7	.22	.49	.27
FOSR Bay 12	.13	.29	.16

The mass deposition measured during ascent by the QCM's is shown in Fig. 12-3. The results are shown in TM volts, but the calibration curves for the QCM's indicate that the actual mass deposit during ascent was 3.8×10^{-5} g/cm^2.

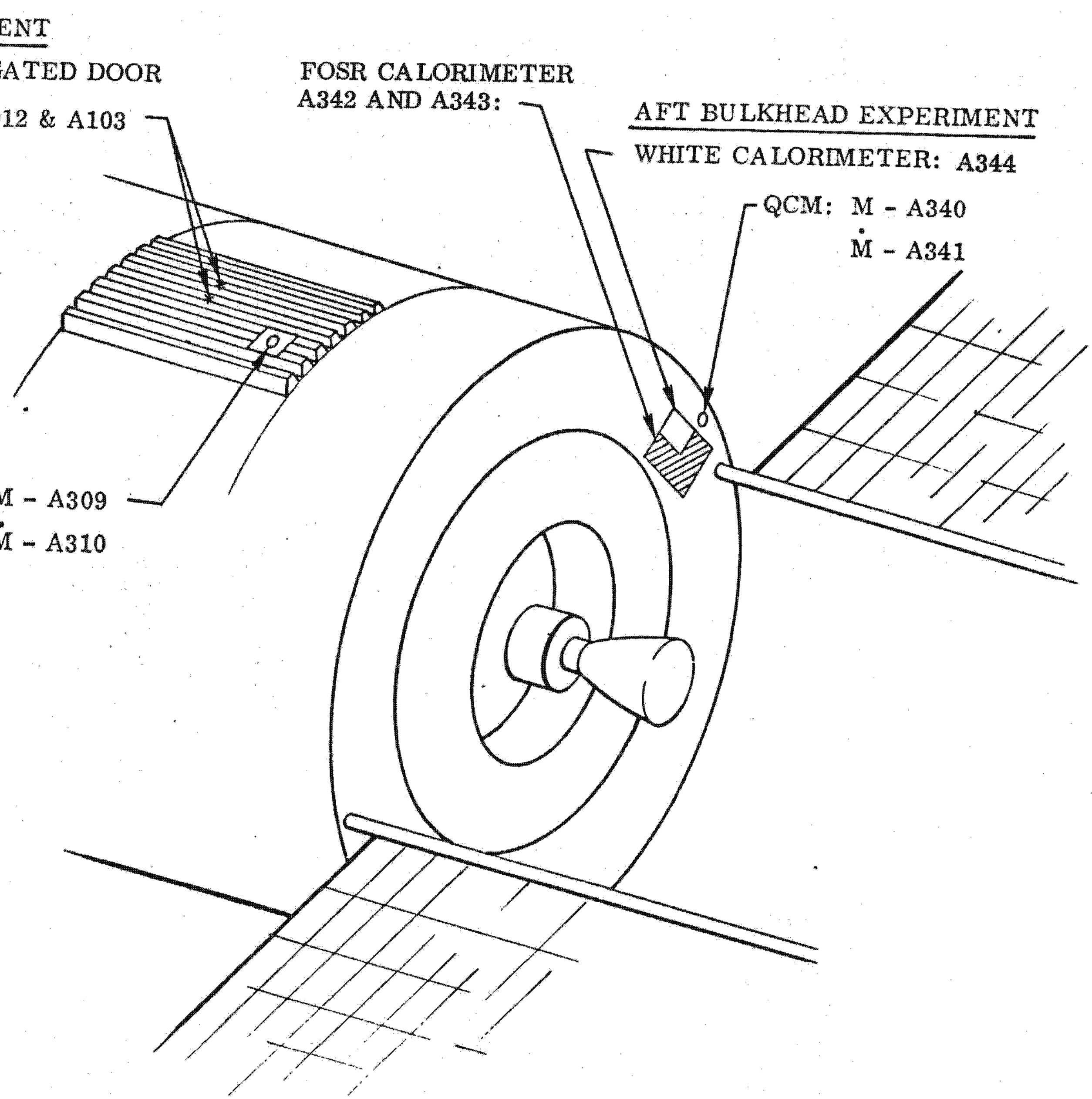

Fig. 12-2 8004 Contamination Experiments

TOP SECRET / H

BIF003W/2-068875-73

Approved for Release: 2021/04/09 C05132862

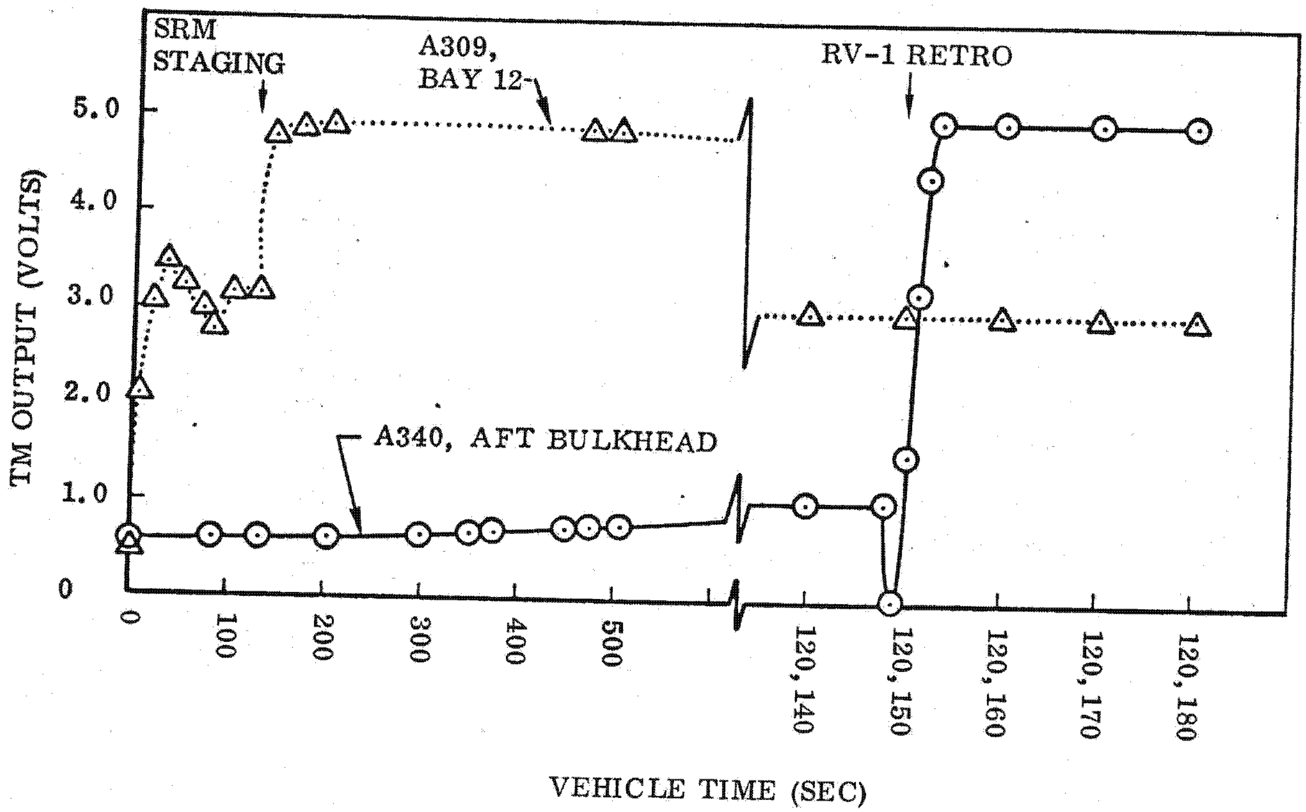

Fig. 12-3 8004 QCM Data

BIF003W/2-068875-73

12.4.2.2 Aft Bulkhead. The ascent contamination caused negligible change in the mass deposition level measured by the Station 2203 QCM as shown in Fig. 12-2. This was as expected, as the SRM staging event causes only a momentary inflow of external gases into the aft section cavity via the vent ports. The first RV retro caused the mass deposit to rise from near lift-off levels to the telemetry limit of 5 TMV where it remained until the second RV retro. The extrapolated mass deposit due to the first RV was 3.8×10^{-5} g/cm^2. The second RV retro caused the QCM to saturate and the crystal stopped oscillating as is expected when the mass deposit becomes excessive. The FOSR and white silicone calorimeter panels indicated an increase in α of 0.10 and 0.13 respectively from early flight to after the RV-3 retro event. After correction for ultraviolet degradation, a total change in α of 0.06 for both calorimeters is associated with the three contamination events.

12.4.3 Conclusions

12.4.3.1 Aft Section – Bay 12. The ascent contamination exhibited the same general characteristics of deposit times and magnitude as did that of SV-2 and -3, and the SRM staging event again caused significant contamination. The total deposit again approached TM saturation and was slightly higher than SV-2 or -3. Again, the dip in indicated mass deposit between 60 and 100 seconds after lift-off is caused by temperature gradients induced in the QCM during ascent aeroheating and does not indicate an actual mass loss. Orbital temperature data indicates that the FOSR tape successfully survived the ascent environments and experienced only about half the contamination degradation that areas of white paint experienced.

12.4.3.2 Aft Bulkhead. The mass deposition due to RV retro plume impingement generally agreed with analytical predictions (3.8×10^{-5} g/cm^2 measured per RV vs. 2.8×10^{-5} g/cm^2 predicted). The somewhat unexpected result was that this mass deposit caused an average change in α of 0.02 per RV for white silicone paint whereas the same deposit on the aft section during SRM staging caused a 0.30 change in α. This result can be tentatively explained by theorizing that the mean particle size of the contaminating material produced during SRM staging (aluminum oxide particles plus miscellaneous solids from the BV insulator pad) is significantly smaller than the particles produced by the RV retro motors (almost 100% aluminum oxide). A given mass of small particles will cover more surface area, hence cause larger changes in α than the same mass of large particles.

A specific objective of the aft bulkhead experiment was to measure the contamination environment expected on the Quantic experiment scheduled for SV-8. The Quantic equipment installation was designed with shields to protect against the contaminants and the results reported above confirm that this protection is indeed mandatory.

12.4.4 Action for Subsequent Vehicles

FOSR is now considered to be fully qualified for flight and its extensive use in lieu of white silicone paint is being implemented for aft section external surfaces on SV-5 and up.

No further contamination experiments are planned.

Section 13
MASS PROPERTIES

The history of the SV mass properties throughout the flight are tabulated in Table 13.1.

Table 13-1

SV-4 MASS PROPERTIES

Description	Weight (lb)	Center of Gravity (inches)			Moment of Inertia (slug-ft^2)			Product of Inertia (slug-ft^2)		
		SV Sta	Y	Z	I_x	I_y	I_z	I_{xy}	I_{xz}	I_{yz}
After Injection	19630	2005.4	1.53	4.08	4663	128600	128298	-163	1835	-125
Solar Arrays Extended	19630	2005.9	1.53	4.08	5819	129602	130400	-160	1843	-347
After Subsat Ejection	19501	2002.2	1.28	4.25	5757	128569	129347	-362	1985	-319
Before Drop 1	19281	1996.5	1.34	4.91	5726	135937	136721	-458	2442	-332
After Drop 1	17751	2024.0	1.46	3.82	5519	99040	99968	-305	999	-326
Before Drop 2	17157	2007.6	1.65	4.83	5460	102744	103686	-483	1298	-356
After Drop 2	15613	2036.1	1.81	3.57	5247	76222	77309	-321	50	-348
Before Drop 3	15208	2024.4	1.86	4.25	5282	78780	79827	-390	474	-352
After Drop 3	13697	2048.4	2.07	2.78	5067	61358	62555	-245	-572	-343
Before Drop 4	13251	2037.4	2.14	3.62	5087	61961	63122	-314	-299	-349
After Drop 4	11754	2058.5	2.41	1.88	4869	51730	53042	-184	-1123	-338
Prior to Deboost	10958	2049.1	2.71	2.22	4831	48588	49913	-282	-1238	-352
After Deboost	10630	2044.5	2.79	2.29	4828	47017	48342	-310	-1261	-353

~~TOP SECRET / H~~

66

~~TOP SECRET / H~~

BIF003W/2-068875-73

Section 14
STRUCTURE AND DYNAMICS

14.1 PRELAUNCH WINDS ALOFT LOADS ANALYSIS

Table 14-1 presents a chronological tabulation of the winds aloft computer runs for SV-4. The results are plotted on Fig. 14-1.

The loads and control analysis computer simulations leading to launch were accomplished without violating any of the established vehicle constraints and resulted in repeated Go for Launch recommendations.

An R-17 day preliminary winds loads data check run was accomplished on 27 September 1972. These data checked the Martin Marietta (MMC) and the Vandenberg Targeting Team (VTT) independently generated data well within the acceptable limits. MMC verified the SBAC data results as being correct on 28 September 1972 by letter (MMC 72-Y-32004).

14.2 SOLAR ARRAY

The erections and deployment time histories for both the left (-Y) and right (+Y) solar arrays are shown in Fig. 14-2. Since the arrays were deployed and erected in the proper position for the flight beta angle, no positioning was necessary and none was performed during the basic mission. Positioning to the standard positions of ±18 and 0 degrees were accomplished on both arrays during the SOLO mission.

The times for deployment and erection of the left array were similar to those for previous vehicles. The right array indicated that some motion was experienced by the deployment potentiometer at the time of the command but then no motion occurred for 28 minutes. The right array then deployed and erected in a normal manner. The

Table 14-1

WINDS ALOFT ANALYSIS SUMMARY

	Balloon Release Time				
	T-30	T-12	T-6	T-3	T-0
	3800 Run at STC Time				
	T-24	T-8.5	T-3	T-1	---
SV Structural Loads:					
Bending Mom, % Limit Load	70.34	82.13	76.10	77.80	67.23
Critical SV Station	1902	1902	1902	1902	1902
Elapsed Time (seconds)	54.9	55.6	51.5	52.3	56.1
Altitude (feet)	33,998	34,898	29,994	31,002	35,449
SRM Side Force:					
% Allowable	42.84	61.19	50.41	55.3	66.2
SRM No.	1	1	1	1	2
Pitch or Yaw	Pitch	Pitch	Pitch	Pitch	Pitch
TVC Usage for Control:					
% Allowable Expended	63.0	59.8	69.3	63.9	60.0
SRM No.	1	1	1	1	1
Expended (pounds)	1338.9	1275.9	1477.0	1358.9	1275.3
Vehicle Response:					
Maximum αq, % allowable	42.38	49.66	44.54	46.12	29.68
Maximum αq, deg-psf	1325.9	2086.8	1904.4	1985.0	985.5
Elapsed Time (seconds)	36.6	56.5	51.5	52.3	70.5
Altitude (feet)	14,998	36,010	29,994	31,002	55,693

~~TOP SECRET~~ / ~~H~~

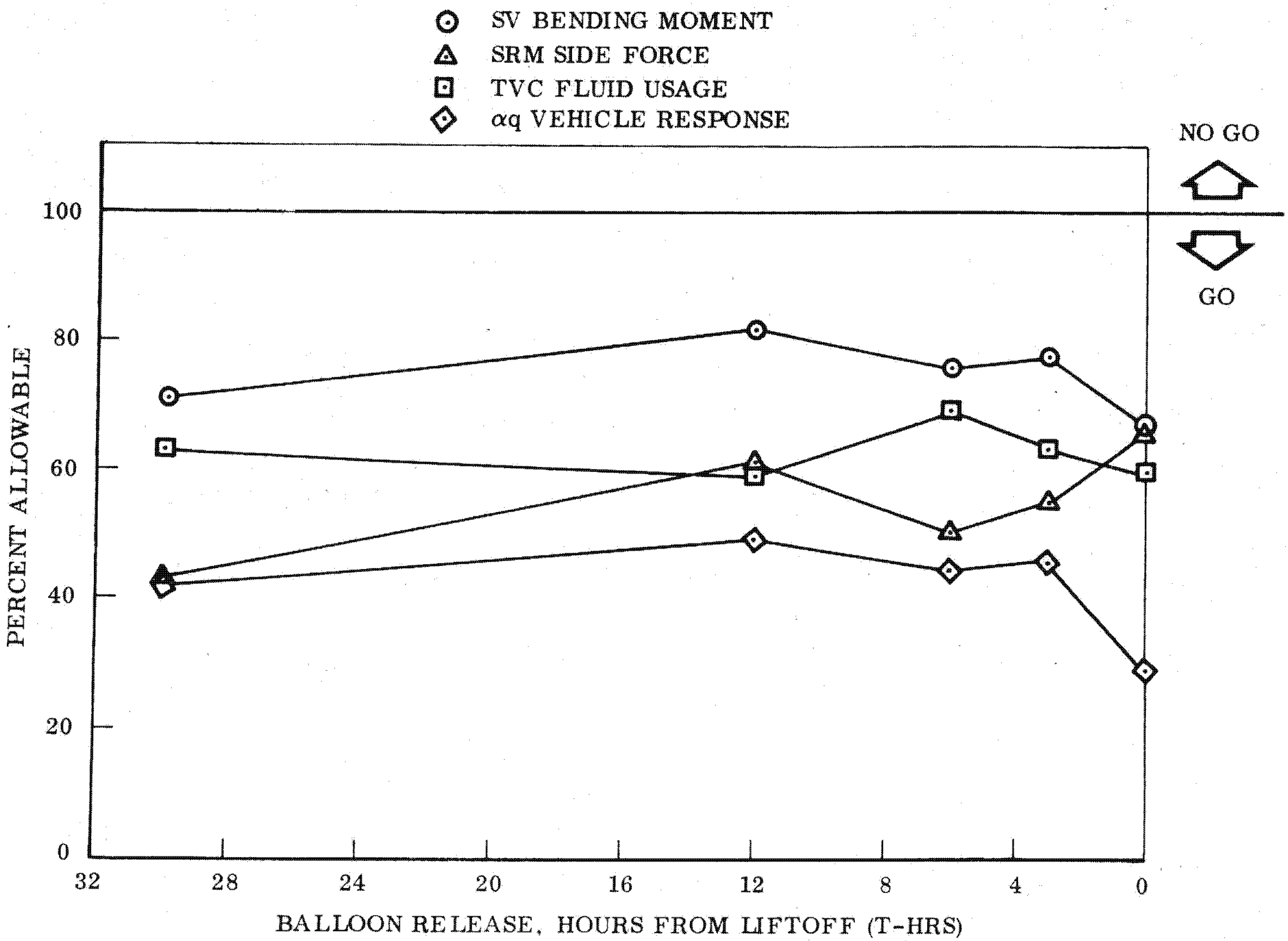

Fig. 14-1 Critical Parameter Summary

~~TOP SECRET~~ / ~~H~~

BIF003W/2-068875-73

Approved for Release: 2021/04/09 C05132862

TOP SECRET / H

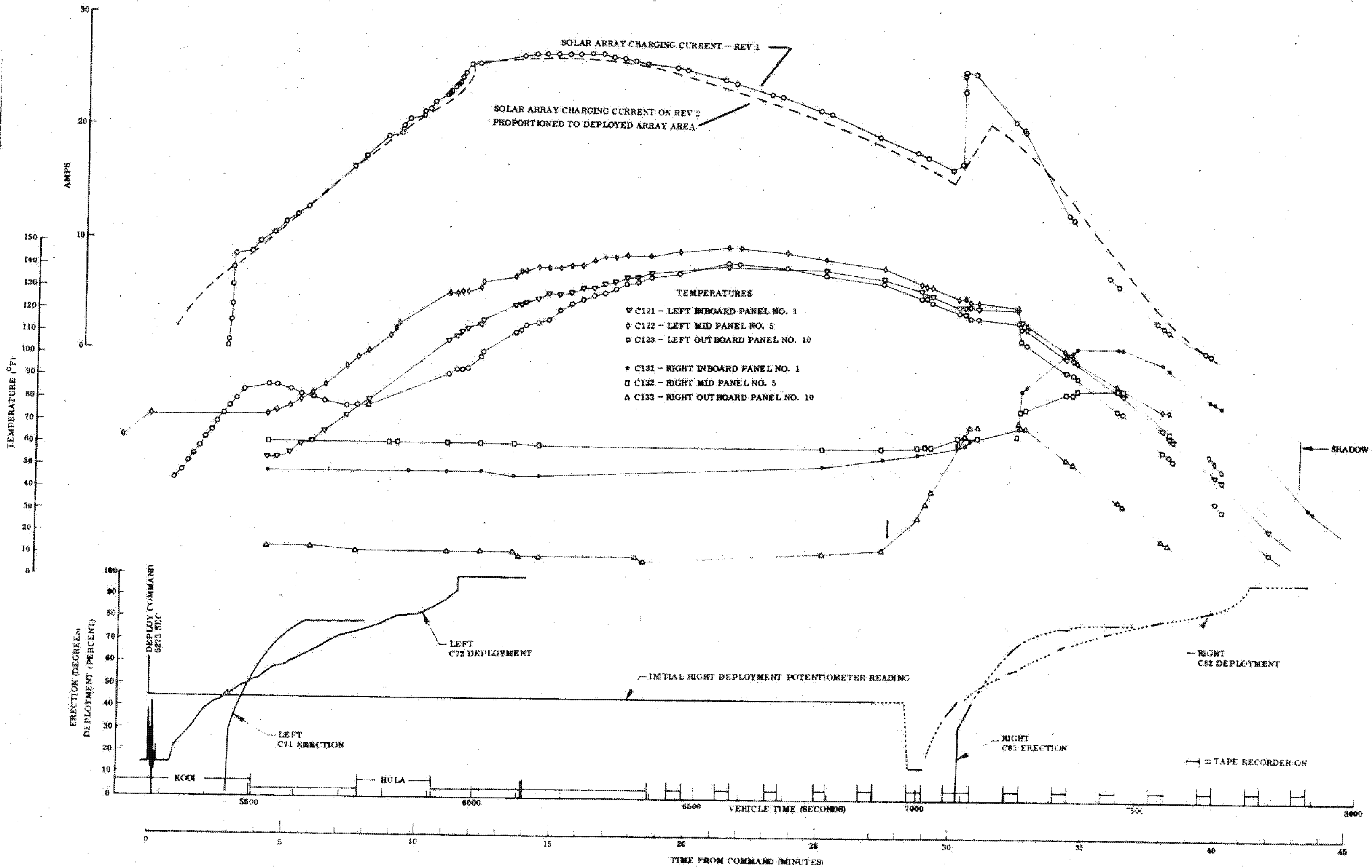

Fig. 14-2 Time History of Solar Array Parameters During Deployment

TOP SECRET / H

BIF003W/2-068875-73

delay was attributed to the sticking rubber pads added to the restraining cage arms (on SV-4 only) to the white silicone paint on the outer surface of the right array. Heat and plastic deformation of these pads eventually permitted the cage arms to disengage and the subsequent motion was normal. The pads ability to prevent the cage from releasing the array was reproduced in the laboratory.

The conclusion that the right array had not been released by the cage mechanism was deduced from the additional curves shown on Fig. 14-2. The electrical charging current for Rev 1 is shown as is also a curve generated by multiplying the current generated on Rev 2 by the solar array area exposed if the right array followed the postulated deployment. It is interesting to note that the erection motion has to occur before the arrays are in a position to produce energy. Also the temperature of panels 1, 5 and 10 of both arrays are shown and the beginning of deployment can be seen in the rapid rise of the panel 10 sensor. Because of the time delay, the sun angle on the right panel 10 was similar to that on the left panel 10 at the time of deployment, the left being illuminated near sunrise and the right near sunset.

A thorough review of the solar array was conducted and the following changes for SV-5 and subsequent vehicles were implemented:

- The rubber pads at the restraining cage arm tips were removed.
- Teflon blocks have been added to the tips of the two arms which disengage first in the sequence. This will support the solar leaves during ascent (this was the purpose of the rubber pads added on SV-4) but adhesion to the white silicone paint is a minimum and more force is available to move these arms.
- Teflon surfaces are being provided wherever silicone rubber contacted metal or other surfaces that could produce forces working against the solar array motion.
- A spring has been added between panels 10 and 11 on the right array to prevent a theoretically possible overcenter interference.
- Instrumentation has been added to aid in analyzing the solar array motion in flight.
- Silicone rubber protection of the electrical cabling has been removed which should result in a faster deployment.

In addition to deployment tests in the laboratory, the cage release mechanism of the final flight configuration for SV-5 was demonstrated in a -80°F and vacuum environment.

Section 15
SOFTWARE

There were no software problems which impacted flight objectives.